



1. Introduction

The empirical model developed by Laurenza et al. (2009) based on data from 1995 to 2005, can provide short-term warnings of solar energetic proton (SEP) events that meet or exceed the Space Weather Prediction Center threshold of $J (> 10 \text{ MeV}) = 10 \text{ p cm}^{-2} \text{ s}^{-1} \text{ sr}^{-1}$, within 10 minutes after the maximum of $\geq \text{M2}$ soft X-ray (SXR) flares. We analysed the $\geq \text{M2}$ SXR and type III radio bursts occurred in the period 2006 - 2014 and computed the parameters of the model, i.e. the time-integrated intensity of SXR and of type III radio emission at about 1 MHz. The occurrence of $\geq \text{M2}$ SXR flares is found to be reduced in the investigated period of 40% with respect to that in the period 1995 - 2005. The probability density functions associated with both parameters point out that high values of SXR and radio fluence ($>0.1 \text{ J/m}^2$ and $>5 \times 10^6 \text{ SFU} \times \text{min}$) are noticeably reduced (21% and 23%, respectively), compared to those (33% and 36%, respectively) obtained for 1995 - 2005, especially when SEP associated events are considered. Moreover, in order to test the accuracy of the model, the probability of detection (POD) and the False Alarm Rate (FAR) were evaluated by using the new database. The obtained verification measures show a good performance of the model: $\text{POD} = 59\%$, $\text{FAR} = 30\%$, which are, respectively, comparable and even lower with respect to those obtained from the dataset on which the model was developed. In addition, the performance is very high when major SEP events, having a peak flux $\geq 100 \text{ pfu}$, are considered ($\text{POD}=79\%$, $\text{FAR}=5\%$). i. e., for the most hazardous Space Weather conditions. Finally, the mean warning time (as computed by [2]) was estimated to be $\sim 11 \text{ h}$, highly exceeding that obtained through other competing techniques.

2. Methods

We obtained a representative measure of the X-ray fluence by integrating the X-ray intensity between the 1/3 power point before the X-ray peak and the 1/3 power point after it. Then, a fit, based on the intensity values from 6 to 10 minutes after the peak, was performed to take into account the flare profile for an algorithm designed to run in real time for a short time prognosis of SEP events. The data obtained from the Wind/Waves website shows that, for all the time interval considered, 916 kHz was the closest frequency to 1 MHz at which measurements were routinely made. Because the 1 MHz profiles are more highly structured and less regular than the SXR time-intensity curves, the radio time-integration begins 20 minutes before the time of the 1/3 X-ray peak until 10 minutes after the X-ray peak. An example of the computation of key parameters is shown in Figure 1 for the December 13, 2006 SEP event.

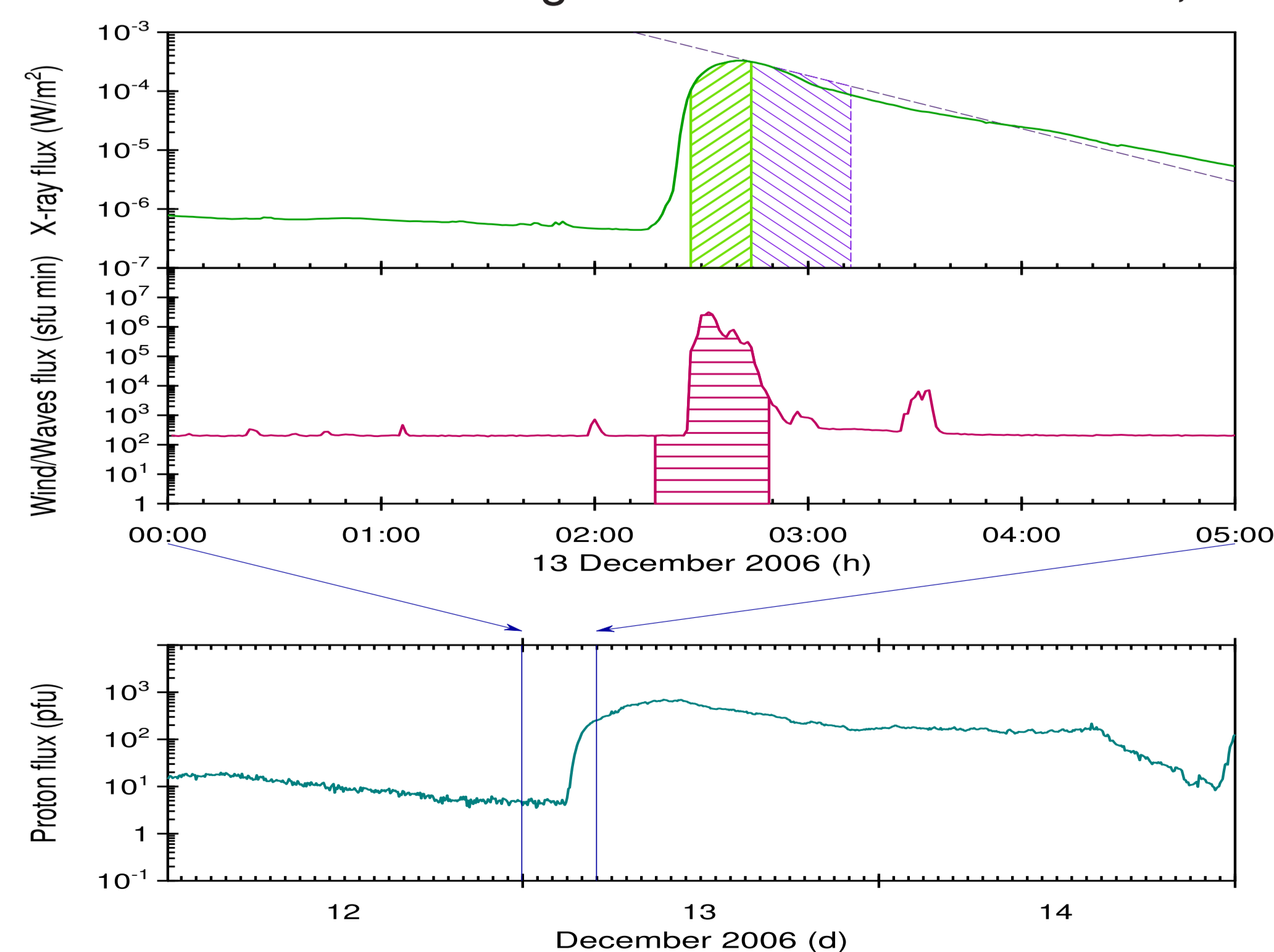


FIGURE 1: December 13, 2006 SEP event. From top to bottom: X-ray flux, Radio Waves flux and Proton flux.

3. Distribution of SXR and Radio Fluence

The probability distribution functions (PDFs) associated with the SXR and the radio fluence can be explored by distinguishing between SEP and non SEP associated events. The empirical PDFs are estimated through the kernel density estimator technique (see Alberti et al. (2014) for more details).

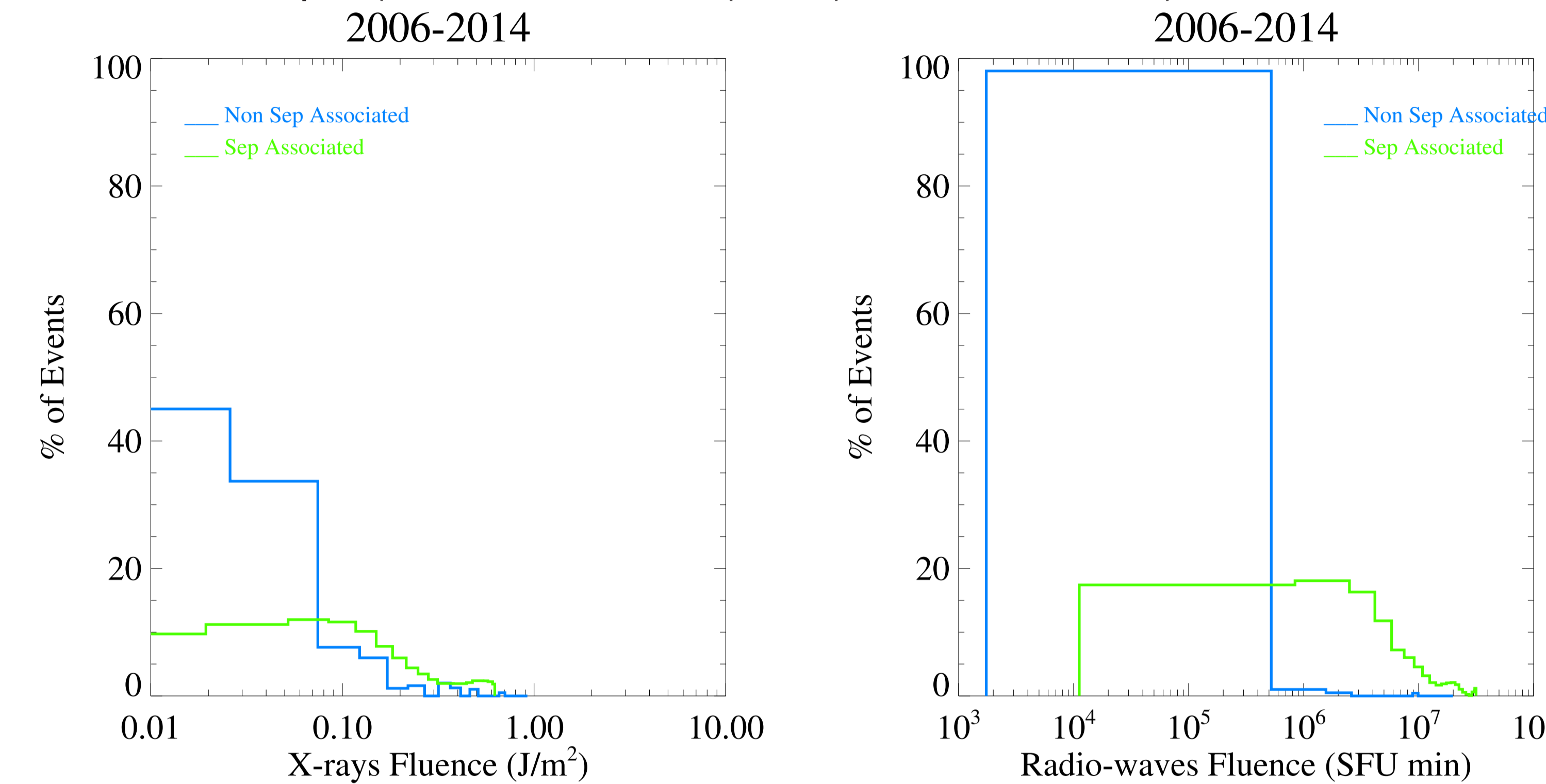


FIGURE 2: SXR fluence [left] and Radio fluence [right] PDFs.

Figure 2 shows that, generally, high values of SXR fluence are found to be associated to SEP events. We note a critical value for the SXR fluence (0.1 J/m^2) above which the percentage of SEP associated (green line in Figure 2, left) $\geq \text{M2}$ X-ray bursts increases to 39% (9/23). On the contrary, the percentage of non SEP associated (blue line in Figure 2, left) $\geq \text{M2}$ X-ray bursts having SXR fluence greater than 0.1 J/m^2 is quite low: 13% (34/253).

Similar results are obtained analyzing PDFs related to 1 MHz radio fluence for both time periods. As shown in Figure 2 (right), the percentage of SEP associated (green line) $\geq \text{M2}$ X-ray bursts having radio fluence greater than $6 \times 10^5 \text{ SFU} \times \text{min}$ is 43% (10/23). Conversely, the percentage of non SEP associated (blue line in Figure 2, right) $\geq \text{M2}$ X-ray bursts having radio fluence greater than $6 \times 10^5 \text{ SFU} \times \text{min}$ is very reduced, i.e. 4% (12/253).

The model developed by [1], is based on the SXR and radio fluence and flare location, to provide short-term warnings of solar energetic proton (SEP) events that meet or exceed the threshold of $J (> 10 \text{ MeV}) = 10 \text{ p cm}^{-2} \text{ s}^{-1} \text{ sr}^{-1}$, within 10 minutes after the maximum of the associated soft X-ray flare. A logistic regression is used to obtain a continuous function for the probability (P) of SEP event occurrence as a function of the SXR (X) and radio (R) fluence as

$$P(\log X, \log R) = \frac{e^{\eta}}{1 + e^{\eta}} \quad (1)$$

where $\eta = \eta(\log X, \log R)$. The accuracy of the model can be investigated by evaluating the Probability of detection (POD) and the False Alarm Rate (FAR), that can be expressed in terms of three values:

1. the number of hits (a SEP event was forecast and one occurred) which we named A
2. the number of false alarms (a SEP was forecast but none occurred) named B
3. the number of missed events (no SEP event was predicted but one occurred) named C

In this way,

$$\text{POD} = \frac{A}{A + C} \quad (2)$$

$$\text{FAR} = \frac{B}{A + B} \quad (3)$$

4. Results of ESPERTA model

In order to test the accuracy of the model, the probability of detection (POD) and the False Alarm Rate (FAR) were evaluated. The obtained verification measures show a good performance of the model: $\text{POD} = 59\%$ and $\text{FAR} = 30\%$, which are, respectively, comparable and even lower with respect to those obtained from the dataset on which the model was developed. Moreover, the performance is very high when major SEP events, having a peak flux $\geq 100 \text{ pfu}$, are not considered ($\text{POD}=79\%$, $\text{FAR}=5\%$), i.e., for the most hazardous Space Weather conditions.

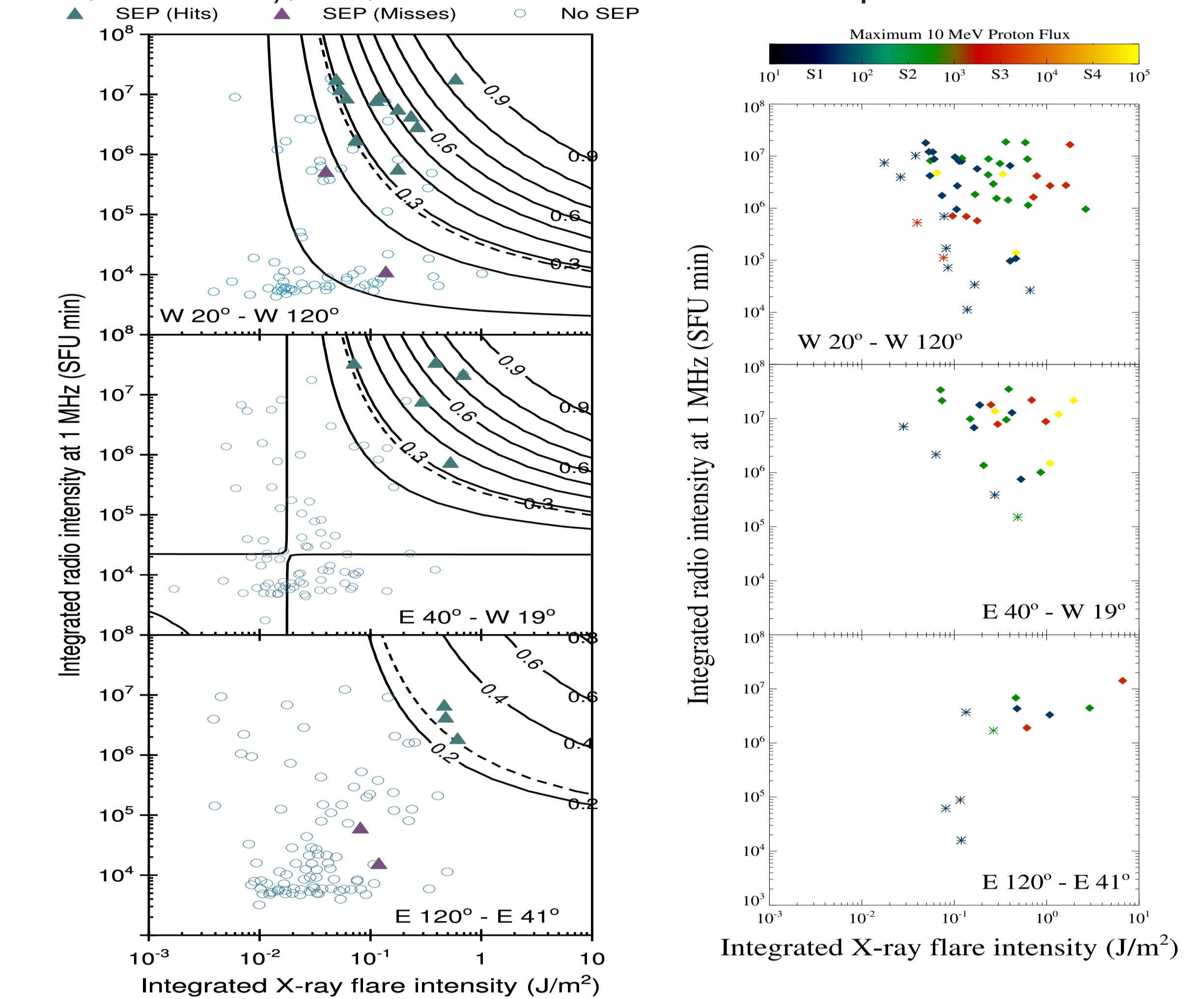


FIGURE 3: [Left] Probability contours for SEP forecasting for three different longitudinal bands: SEPs hit (green triangles), SEPs miss (violet triangles) and No SEPs associated (circles). [Right] Distribution of SEP peak flux for Hits (diamonds) and Misses (stars).

5. Discussion

We found that, even though solar activity was low during the growth and maximum phase in cycle 24, the percentage of $\geq \text{M2}$ X-ray bursts associated with SEP events is observed to be about the same (75/704 and 23/276) with respect to the database used in [1].

We found that the POD level is almost the same of that obtained in [1], indicating a non-dependence of the probability of occurrence by the choice of the datasets but only by the solar parameters related to the X-ray and radio fluence. This is a relevant result because our model is able to give reliable prediction results from the conditions in which SEPs are generated.

Conversely, the FAR level is lower with respect to [1], indicating an improvement of the performance of the model. Moreover, we found that the POD is highly increased (81% - 44/54) for the most hazardous SEP events ($> \text{S1}$, i.e. proton flux $\geq 100 \text{ pfu}$) and that our model is able to predict, with a high level of POD, SEP events characterized by high values of integrated X-rays flare intensity and integrated radio intensity. In conclusion, the merits of ESPERTA are that a good performance is achieved before particles of any energy arrive at the Earth and that it is able to predict, with a high level of POD, SEP events characterized by high values of integrated X-rays flare intensity and integrated radio intensity (see Figure 3), i.e. the most dangerous Space Weather condition.

References

1. Laurenza, M. et al. 2009, Space Weather, 7, S04008, doi:10.1029/2007SW000379.
2. Nunez, M. 2011, Space Weather, 9, S07003
3. Alberti, T. et al 2014, Clim of the Past , 10, 1751